NASA

Technical Memorandum 85025

# Relationships Between Field-Aligned Currents, Electric Fields, and Particle Precipitation as Observed by Dynamics Explorer-2

**M. Sugiura, T. Iyemori, R. A. Hoffman, N. C. Maynard, J. L. Burch, and J. D. Winningham**

**MAY 1983**

National Aeronautics and Space Administration

**Goddard Space Flight Center**
Greenbelt, Maryland 20771

# RELATIONSHIPS BETWEEN FIELD-ALIGNED CURRENTS, ELECTRIC FIELDS, AND PARTICLE PRECIPITATION AS OBSERVED BY DYNAMICS EXPLORER-2

M. Sugiura, T. Iyemori, R. A. Hoffman, N. C. Maynard
Goddard Space Flight Center, Greenbelt, Maryland 20771

J. L. Burch, J. D. Winningham
Southwest Research Institute, San Antonio, Texas 78284

MAY 1983

## ABSTRACT

The relationships between field-aligned currents, electric fields, and particle fluxes are determined using observations from the polar orbiting low-altitude satellite Dynamics Explorer-2. It is shown that the north-south electric field and the east-west magnetic field components are usually highly correlated in the field-aligned current regions. This proportionality observationally proves that the field-aligned current equals the divergence of the height-integrated ionospheric Pedersen current in the meridional plane to a high degree of approximation. As a general rule, in the evening sector the upward field-aligned currents flow in the boundary plasma sheet region and the downward currents flow in the central plasma sheet region. The current densities determined independently from the plasma and magnetic field measurements are compared. Although the current densities deduced from the two methods are in general agreement, the degree and extent of the agreement vary in individual cases.

## INTRODUCTION

Field-aligned currents, electric fields, and precipitating particle fluxes constitute key physical parameters in the magnetosphere-ionosphere coupling processes. Theoretical models for a self-consistent system of this coupling mechanism have been presented by Vasyliunas (1970, 1972), Wolf (1970, 1974), Harel et al. (1979) and many others. Extensive studies have been made on the relationships between field-aligned currents, electric fields, and particle precipitation using data from satellites, sounding rockets, and ground-based facilities. Bostrom (1974) theoretically recognized the proportionality between the electric and magnetic field components associated with field-aligned currents and pointed out the resemblance between some of the magnetic field signatures of field-aligned currents observed by Triad (Armstrong, 1974) and some of the electric field variations observed from Injun 5 (Gurnett and Frank, 1973), although the comparison was not between simultaneously observed data. Comparisons of simultaneous magnetic and electric field signatures of field-aligned currents have been made using the electric and magnetic field observations on the S3-2 and S3-3 satellites (e.g., Burke et al., 1980; Smiddy et al., 1980; Rich et al., 1981), the ion drift and magnetic field measurements on AE-C (Bythrow et al., 1980), the Chatanika radar observations (e.g., de la Beaujardiere et al., 1977), and a combination of the Chatanika radar observations and the magnetometer measurements from Triad, (e.g., Robinson et al., 1982).

Early investigations of the relations between auroral particle precipitation and field-aligned currents (and also electric fields) are reviewed by Arnoldy (1974) and Anderson and Vondrak (1975). Numerous papers have been written on this subject since then, using particle flux measurements or optical observations of the aurora and the field-aligned current data deduced from magnetic field measurements or from incoherent scatter radar observations (e.g., Klumpar, 1979; Burke et al., 1980; Robinson et al., 1982; Senior et al., 1982).

One of the objectives of the Dynamics Explorer (DE) mission is to

investigate quantitatively the relationships between field-aligned currents, electric fields, and particle fluxes with simultaneous observations. Descriptions of the magnetometer, the electric field probe, and the plasma experiment (LAPI) have been given by Farthing et al. (1981), Maynard et al. (1981), and Winningham et al, (1981), respectively.

## CORRELATION BETWEEN MAGNETIC AND ELECTRIC FIELDS

Sugiura et al. (1982) have presented initial DE-2 results on the correlation between the magnetic and electric fields in the field-aligned current regions. They showed that the traces of the north-south component of the electric field and of the east-west component of the magnetic field are usually very similar and that the correlation coefficient between these parameters is often as high as 0.99. Figure 1 shows the north-south component of the electric field and the geomagnetic north-south and east-west components of the magnetic field observed from DE-2 during a pass on July 29, 1982, 0606-0610UT, crossing the dayside cusp. The x component of the electric field is along the satellite velocity vector and in this case it is northward. The magnetic field data plotted are the differences between the observed field and a reference field based on the latest Magsat model field (see Langel et al., 1980, for a description of the Magsat results). The sampling rate of the measurement is 16 samples per second both for the electric and magnetic field observations. There is a striking similarity between the north-south electric field and east-west magnetic field components except that the electric field data show considerably more rapid fluctuations than the magnetic field data. Using 1/2 second averages, the coefficient of correlation between these two parameters for the 6-minute period 0605 to 0611 (containing the 4-minute interval shown in the figure) is 0.992. To see if the correlation varies significantly between the regions of weak current (equatorward and poleward of the cusp) and the vicinity of the cusp where the current is more intense, the above interval was divided into three segments: 0606:10-0607:30, 0607:30-0609:00, and 0609:00-0610:00, and the correlation coefficient was calculated for each of these segments, using the high time resolution data (at 16 samples per second). The correlation coefficients so calculated are 0.996, 0.98, and 0.98 respectively. This result shows that the high

correlation is not limited to the regions where the current densities are large.

We now examine the relation between the electric and magnetic fields analytically. Let the x, y and z axes be toward the north, east and downward, respectively. For simplicity, let the ambient magnetic field be vertical and downward. We assume that $\partial b_z/\partial t = 0$ and that $b_x$ is independent of y (i.e. $j_{\parallel} = -(1/\mu_0)\partial b_y/\partial x$), where $\underline{b}$ is the perturbation magnetic field, the y component of which corresponds to $\Delta B_\phi$ in our data presentation. Then by equating $j_{\parallel}$ to the divergence of the height-integrated horizontal ionospheric current, we obtain

$$(1/\mu_0)\partial b_y/\partial x = \partial(\Sigma_P E_x)/\partial x + \partial(\Sigma_P E_y)/\partial y + E_x \partial\Sigma_H/\partial y - E_y \partial\Sigma_H/\partial x \qquad (1)$$

where $\Sigma_P$ and $\Sigma_H$ are the height-integrated Pedersen and Hall conductivities. If $E_y$ is independent of x, and if the conductivities and $E_y$ are independent of y, eq.(1) can be integrated to give

$$b_y = \mu_0(\Sigma_P E_x - \Sigma_H E_y) + \text{const} \qquad (2)$$

If the observed values of $b_y$ are linearly correlated with those of $E_x$ with a coefficient of correlation near unity over distances of several hundred or even several thousand kilometers along the x axis, we must conclude either (a) that the north-south Hall current is zero and that

$$b_y = \mu_0 \Sigma_P E_x + \text{const} \qquad (3)$$

or (b) that $E_y$ is always proportional to $E_x$. However, $E_y$ was assumed to be independent of x in deriving eq.(2). Since $E_x$ varies with x, the proportionality of $E_y$ to $E_x$ contradicts with this assumption. Hence (a), i.e. eq.(3), is the only choice.

If eq.(3) holds, then the slope of the $b_y$ (corresponding to $\Delta B_\phi$ in Figure 1) vs. $E_x$ enables us to determine $\Sigma_P$. We have made several simplifying assumptions in deriving the relationship expressed by eq.(3). However, considering the complexity of eq.(1), the probability that the

proportionality between $b_y$ and $E_x$ holds over large distances on many passes at different local times would appear near null if the terms other than the first term are not negligible. We thus conclude that when the correlation between the north-south component of the electric field and the east-west component of the magnetic field is high, the field-aligned current equals the divergence of the height-integrated Pedersen current within the meridional plane, and that the Hall current from an east-west electric field, if any, makes no significant contribution to the field-aligned current under this condition.

For the three subintervals mentioned above in reference to the July 29, 1982 example, the value of $\Sigma_p$ determined by eq.(3) is 5.3, 5.5 and 5.9 mhos, respectively. The variation in $\Sigma_p$ is relatively small even though the current densities vary between these sections. This feature is consistent with the interpretation that the primary source of ionization is the solar EUV, and is in strong contrast with the condition on the nightside where the ionization is mainly from precipitating particles. Sugiura et al.(1982) have shown an example near 21 hours MLT in which the conductivity is largest where the current is most intense and in which the conductivity decreases away from the main current region.

## RELATIONS WITH PARTICLE PRECIPITATION IN EVENING SECTOR

From an extensive inspection of preliminary energy-time spectrograms obtained from LAPI observations, it has become clear that in no local time sectors do the precipitating positive ions consistently play a primary role in carrying downward field-aligned currents. Therefore in this section we only discuss the relations between electron precipitation and field-aligned currents. The morphological relationships between these parameters are complex and depend strongly on local time. In this paper we limit our discussion to the evening sector. Figure 2 shows from top to bottom, plots of the north-south component of the electric field, the dipole north-south and east-west components of the magnetic field, and the electron energy-time spectrogram at zero degree pitch angle and the electron number flux obtained from LAPI, for a high latitutde pass near magnetic local time (MLT) 19 hours on October 20, 1981. Electrons measured are in the energy

range 5 eV to 32 keV. In the basic mode of operation a 32 point energy spectrum is obtained every second. The electric and magnetic field data are 1/2 second averages. Plots of $\Delta B_\phi$ indicate that the upward field-aligned current region extends approximately from 0756:30 to 0758:20, and that a downward current is observed from 0758:20 to about 0759:00. The current directions are schematically indicated by arrows in the figure. The x component of the electric field in Figure 2 (and also in Figure 3 below) is southward. Therefore the coefficient of correlation between $E_x$ and $\Delta B_\phi$ has an opposite sign to the case shown in Figure 1. The terminology of Winningham et al. (1975) has been found helpful in determining the relationships between the characteristics of electrons and field-aligned currents. According to Winningham et al. (1975), the electron flux precipitating from the central plasma sheet (CPS) is relatively stable with respect to 'substorm time' and spatially uniform, and its variation, if any, is a uniform increase or decrease in intensity. The boundary plasma sheet (BPS) precipitation is characterized by highly variable plasma precipitation poleward of the CPS region. It is in the BPS region that structures such as the 'inverted V' are observed, as seen in the figure. As to the field-aligned currents, it is more convenient for the present purpose to categorize the field-aligned current regions simply by upward and downward current regions rather than by regions 1 and 2 as is usually done following the nomenclature of Iijima and Potemra (1976).

In Figure 2 the upward field-aligned current region coincides with the inverted V's in the boundary plasma sheet (BPS) precipitation and the downward current region is inside the central plasma sheet (CPS). In this example there is a sharp transition between the two main current regions. The spectrogram and the number flux show that the higher electron flux (roughly from 0757:55 to 0758:20) gives a steeper slope in $\Delta B_\phi$ and hence a greater current density. The current density distribution for this pass is given in the next section (Fig. 7).

Another example is presented in Figure 3 for an evening pass near 21 hours MLT on October 29, 1981. From $\Delta B_\phi$, the upward field-aligned current region is approximately from 2324:00 to 2325:40 and is in the BPS electron precipitation region. However, in this example the BPS extends poleward

beyond the high latitude edge of the upward current region and into a region of weak predominantly downward current. As in the previous case of October 20, the abrupt (equatorward) termination of the BPS electons clearly coincides with the boundary between the regions of upward and downward field-aligned current. Again the downward current region roughly coincides with the CPS region.

In the October 29 case there are fine structures in both upward and downward current regions. (The current density profile is shown in Fig. 5 in the following section.) Corresponding to each structure of intensified electron flux, an indication of upward current is discernible in the magnetic field data. This feature is not limited to the evening sector but is common at all local times.

In the electron spectrograms, narrow gaps of varying width are often found which have appearances of 'holes' in the electron precipitation. In these 'holes' the currents are always downward. As an example, referring to Figure 2, a small downward current exists in the BPS region for about 5 seconds after 0757:50, and the electron precipitation nearly vanishes. Another example is seen near 2325:10 in the October 29 event shown in Figure 3.

In these two examples the north-south component of the electric field is generally similar to the east-west component of the magnetic field on large scales but there are appreciable deviations from the proportionality in small scale structures in the evening sector. However, generally speaking, the electric and magnetic field variations are consistent in the manner discussed in the preceding section and in our previous paper (Sugiura et al., 1982).

## CURRENT DENSITIES

The density of field-aligned current is calculated from the east-west component of the magnetic field assuming a series of field-aligned infinite current layers that are locally normal to the dipole meridian plane. The differentiation of the magnetic field component is made with respect to the

distance normal to the current sheets. The current density profile for the cusp pass on July 29, 1982 (Fig. 1) based on 2-second averages of $\Delta B_\phi$ is shown in Figure 4. Even with these smoothed data the current density has large fluctuations. Through a careful examination of the current densities derived from high time-resolution magnetic field data that are not averaged and from averages over various time lengths (1/2 sec, 1 sec, 2 sec, etc.) we have concluded that in terms of current density the field-aligned currents have much more detailed structures than the human eye can resolve in the magnetic field plots. Figure 5 shows the current density plotted with the electric and magnetic field components for the October 29, 1981 pass (Fig. 3). The current density given here is based on 1-second averages of $\Delta B_\phi$, while the electric and magnetic field data are 1/2 second averages as in Figure 3. The maximum current density in the time interval shown is about 10 $\mu A/m^2$.

Figure 6 gives the current density (1-second averages) and the electric and magnetic field components (1/2-second averages) for a pass near 20 hours MLT on October 7, 1981. In this case there was a very thin upward current layer coinciding with a narrow intense BPS electron flux region (electron spectrogram not shown in this paper). The region of irregular current roughly coincides with the CPS region. However, a detailed analysis of plasma data is required to specify the nature of the electron population that is related to the irregular field-aligned currents. There is a region of high electric field with a peak intensity of 150 mV/m near 1029:35, which is an example of a rapid subauroral ion drift (SAID) region (see Spiro et al., 1978). Because of low conductivity, however, the field-aligned current is weak with a current density of only a few $\mu A/m^2$.

A method has been developed to deduce the current density from the plasma measurements on DE-1 and -2 (Burch et al., 1983) on a routine basis. An example of comparison between the current density distributions derived from the LAPI data and from the magnetic field data is shown in Figure 7 for the October 20, 1981 pass (Fig. 2). The energy sweep in LAPI takes 1 second; therefore 1 second is the time resolution in the current density calculation using the LAPI data. Correspondingly, the current density from

the magnetic field data is based on 1-second averages of the field. The overall features are remarkably similar between the two current profiles in the region of upward current, even for small variations. In the region of negative (downward) current, the LAPI currents go nearly to zero. The boundaries of the upward and downward current regions derived from the two methods agree exactly. In this example the current densities determined from the plasma data are generally smaller than those determined from the magnetic field data by factors of 2 to 4. However, this is not always the case; there are examples in which the current densities derived from the magnetic field are smaller than those from the plasma data. There are also cases where the agreement is nearly perfect in some portions of a pass but is rather poor in other portions. These facts indicate an extreme complexity of the relationships between field-aligned currents and particle precipitation. In deriving the current density from the magnetic field data we assumed infinite current sheets. However, this is an idealization and in reality, structured field-aligned currents are more likely to be filamentary (or of irregular shape) than being longitudinally uniform, as for instance the Ogo 4 observations suggested (Berko et al., 1975). Also the time unit of 1-second used is the time required for the plasma instrument to sweep the 32 energy steps, while the 1-second magnetic field data are true averages. The differences between the values of current density derived from the plasma data and from the magnetic field data may partially stem from the different nature of the data. Thus, future studies would require more detailed investigations of the current distribution taking these factors into consideration.

## CONCLUSIONS

With the DE-2 observations the relationships between electric fields, field-aligned currents, and precipitating particles were examined. The north-south component of the electric field and the east-west component of the magnetic field are generally highly correlated in the field-aligned current regions. This high correlation gives an observational proof that the field-aligned current equals the divergence of the height-integrated Pedersen current within the meridional plane to a high degree of approximation. The height-integrated Pedersen conductivity can be

determined from the constant of proportionality between these parameters. In the evening sector the upward field-aligned currents are usually in the boundary plasma sheet region and the downward currents flow in the central plasma sheet region. The current densities calculated from the plasma data and the magnetic field data agree in general features but the magnitudes of the current density determined by the two methods are not necessarily in agreement. The current density distribution has much more detailed structures than is visible to the eye in the magnetic field plots.

Acknowledegements. We wish to thank K. Babst, J. Byrnes, B. Carroll, S. Kempler, A. Meyers, L. Salter, and J. R. Thieman for their assistance in the preparation of this paper. The work at the Southwest Research Institute was supported by NASA Contracts NAS5-26363 and NAS5-2693.

## REFERENCES

Anderson, H. R., and R. R. Vondrak, Observations of Birkeland currents at auroral latitudes, Rev. Geophys. Space Phys., 13, 243, 1975.

Armstrong, J. C., Field aligned currents in the magnetosphere, in Magnetospheric Physics, B. M. McCormac, ed., D. Reidel Publishing Company, Dordrecht-Holland, p.155, 1974.

Arnoldy, R. L., Auroral particle precipitation and Birkeland currents, Rev. Geophys. Space Phys., 12, 217, 1974.

Berko, F. W., R. A. Hoffman, R. K. Burton, and R. E. Holzer, Simultaneous particle and field observations of field-aligned currents, J. Geophys. Res., 80, 37, 1975.

Bostrom, R., Ionosphere-magnetosphere coupling, in Magnetospheric Physics, B. M. McCormac, ed., D. Reidel Publishing Company, Dordrecht-Holland, p.45, 1974.

Burch, J. L., P. H. Reiff, and M. Sugiura, Upward electron beams measured by DE-1: A primary source of dayside region-1 Birkeland currents, in preparation, 1983.

Burke, W. J., D. A. Hardy, F. J. Rich, M. C. Kelley, M. Smiddy, B. Schuman, R. C. Sagalyn, R. P. Vancour, P. J. L. Widman, and S. T. Lai: Electrodynamic structure of the late evening sector of the auroral zone, J. Geophys. Res., 85, 1179, 1980.

Bythrow, P. F., R. A. Heelis, W. B. Hanson, and R. A. Power, Simultaneous observations of field-aligned currents and plasma drift velocities by Atmosphere Explorer C, J. Geophys. Res., 85, 151, 1980.

de la Beaujardiere, O., R. R. Vondrak, and M. Baron, Radar observations of electric fields and currents associated with auroral arcs, J. Geophys. Res., 82, 5051, 1977.

Farthing, W. H., M. Sugiura, B. G. Ledley, and L. J. Cahill, Jr., Magnetic field observations on DE-A and -B, Space Sci. Instr., 5, 551, 1981.

Gurnett, D. A., and L. A. Frank, Observed relationships between electric fields and auroral particle precipitation, J. Geophys. Res.,78, 145, 1973.

Harel, M., R. A. Wolf, P. H. Reiff, and M. Smiddy, Computer modeling of events in the inner magnetosphere, in Quantitative Modeling of Magnetospheric Processes, W. P. Olson, ed., American Geophysical Union, Washington, D. C., p.499, 1979.

Iijima, T., and T. A. Potemra, The amplitude distribution of field-aligned currents at northern high latitudes observed by Triad, J. Geophys. Res., 81, 2165, 1976.

Klumpar, D. M., Relationships between auroral particle distributions and magnetic field perturbations associated with field-aligned currents, J. Geophys. Res., 84, 6524, 1979.

Langel, R. A., R. H. Estes, G. D. Mead, E. B. Fabiano, and E. R. Lancaster, Initial geomagnetic field model from MAGSAT vector data, Geophys. Res. Lett., 7, 793, 1980.

Maynard, N. C., E. A. Bielecki, and H. F. Burdick, Instrumentation for vector electric field measurements from DE-B, Space Sci. Instr., 5, 523, 1981.

Rich, F. J., C. A. Cattell, M. C. Kelley, and W. J. Burke, Simultaneous observations of auroral zone electrodynamics by two satellites: Evidence for height variations in the topside ionosphere, J. Geophys. Res., 86, 8929, 1981.

Robinson, R. M., R. R. Vondrak, and T. A. Potemra, Electrodynamic properties of the evening sector ionosphere within the region 2 field-aligned current sheet, J. Geophys. Res., 87, 731, 1982.

Senior, C., R. M. Robinson, and T. A. Potemra, Relationship between field-aligned currents, diffuse auroral precipitation and the westward electrojet in the early morning sector, J. Geophys. Res., 87, 10469, 1982.

Smiddy, M., W. J. Burke, M. C. Kelley, N. A. Saflekos, M. S. Gussenhoven, D. A. Hardy, and F. J. Rich, Effects of high-latitude conductivity on observed convection electric fields and Birkeland currents, J. Geophys. Res., 85, 6811, 1980.

Spiro, R. W., R. A. Heelis, and W. B. Hanson, Ion convection and the formation of the mid-latitude F region ionization trough, J. Geophys. Res., 83, 4255, 1978.

Sugiura, M., N. C. Maynard, W. H. Farthing, J. P. Heppner, B. G. Ledley, and L. J. Cahill, Jr., Initial results on the correlation between the magnetic and electric fields observed from the DE-2 satellite in the field-aligned current regions, Geophys. Res. Lett., 9, 985, 1982.

Vasyliunas, V. M., Mathematical models of magnetospheric convection and its coupling to the ionosphere, in Particles and Fields in the Magnetosphere, B. M. McCormac, ed., D. Reidel Publishing Company, Dordrecht-Holland, p.60, 1970.

Vasyliunas, V. M., The interrelationship of magnetospheric processes, in Earth's Magnetospheric Processes, B. M. McCormac, ed., D. Reidel Publishing Company, Dordrecht-Holland, p.29, 1972.

Winningham, J. D., F. Yasuhara, S.-I. Akasofu, and W. J. Heikkila, The latitudinal morphology of 10-eV to 10-keV electron fluxes during magnetically quiet and disturbed times in the 2100-0300 MLT sector, J. Geophys. Res., 80., 3148, 1975.

Winningham, J. D., J. L. Burch, N. Eaker, V. A. Blevins, and R. A. Hoffman, The low altitude plasma instrument (LAPI), Space Sci. Instr., 5, 465, 1981.

Wolf, R. A., Effects of ionospheric conductivity on convective flow of plasma in the magnetopshere, J. Geophys. Res., 75, 4677, 1970.

Wolf, R. A., Calculations of magnetospheric electric fields, in Magnetospheric Physics, B. M. McCormac, ed., D. Reidel Publishing Company, Dordrecht-Holland, p.167, 1974.

## FIGURE CAPTIONS

FIGURE 1. The component of the electric field along the spacecraft velocity vector (northward on this pass) and the southward and eastward components of the perturbation magnetic field in geomagnetic diple coordinates, on a dayside cusp pass on July 29, 1982. The height-integrated Pedersen conductivity, $\Sigma_P$, is ggiven for the three segments indicated.

FIGURE 2. The component of the electric field along the spacecraft velocity vector (southward on this pass), the southward and eastward components of the perturbation magnetic field in geomagnetic dipole coordinates, and the energy-time spectrogram and the number flux for electrons, on an evening pass on October 20, 1981. Arrows in the third panel schematically indicate field-aligned current directions.

FIGURE 3. The components of the electric and magnetic fields and tne electron spectrogram and number flux (see Fig. 2 caption) for an evening pass on October 29, 1981.

FIGURE 4. The current density (upper panel) deduced from 2-second averages of the magnetic field data (lower panel) for the cusp pass on July 29, 1981, shown in Fig. 1.

FIGURE 5. The current density (1-second averages) and the electric and magnetic field components (1/2-second averages) for the evening pass on October 29, 1981, shown in Fig. 3.

FIGURE 6. The current density (1-second averages) and the electric and magnetic field components (1/2-second averages) for an evening pass on October 7, 1981. The electric field, $E_x$, plot shows a large electric field in a rapid subauroral ion drift convection region near $60^o$ invariant latitude.

FIGURE 7. Comparison of the current density, $J^{(P)}$, deduced from the plasma data and the current density, $J^{(M)}$, deduced from the magnetic field data; these values are computed once in each second. The bottom panel gives the magnetic field component from which the current density was deduced.

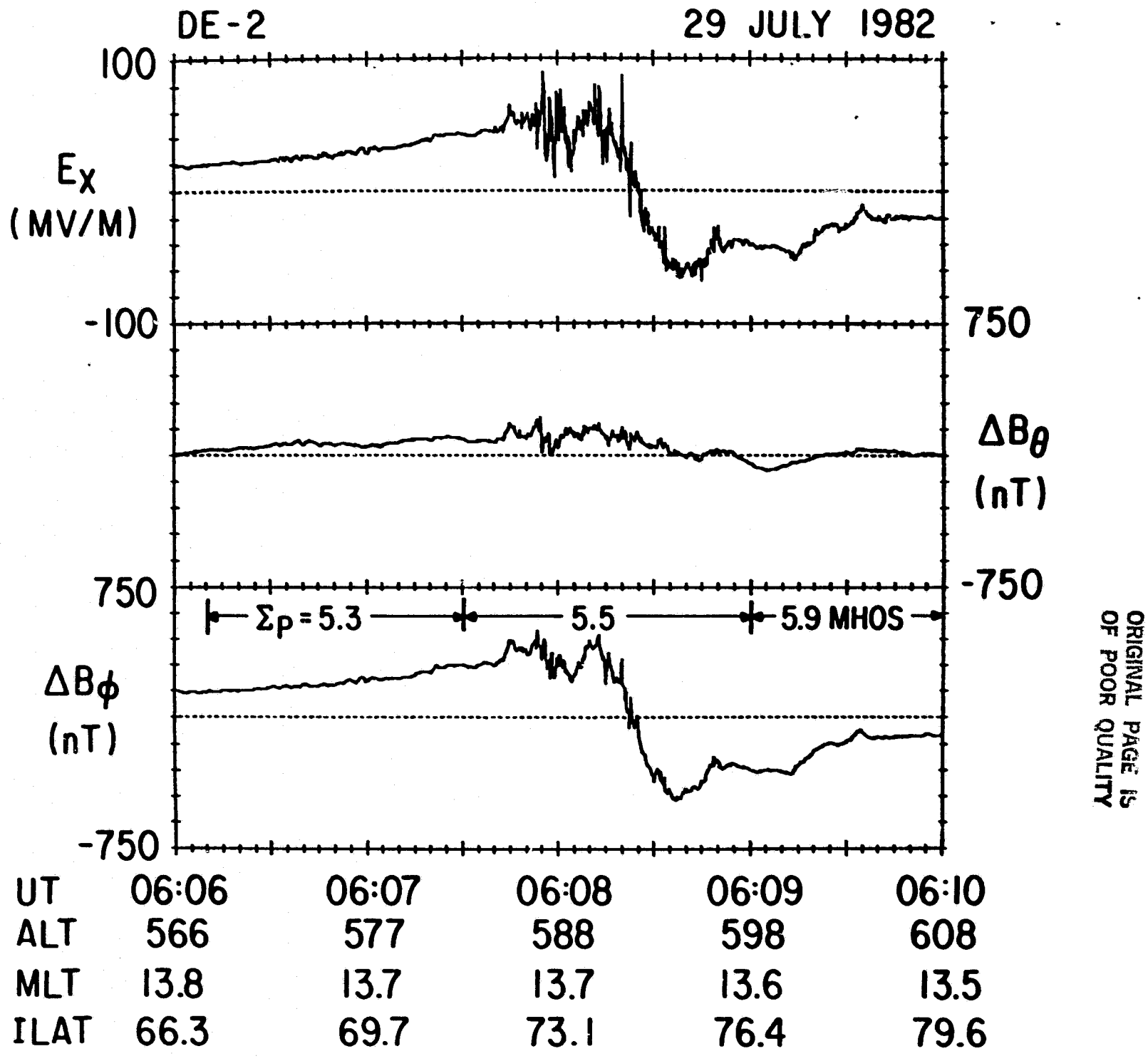




FIGURE 1

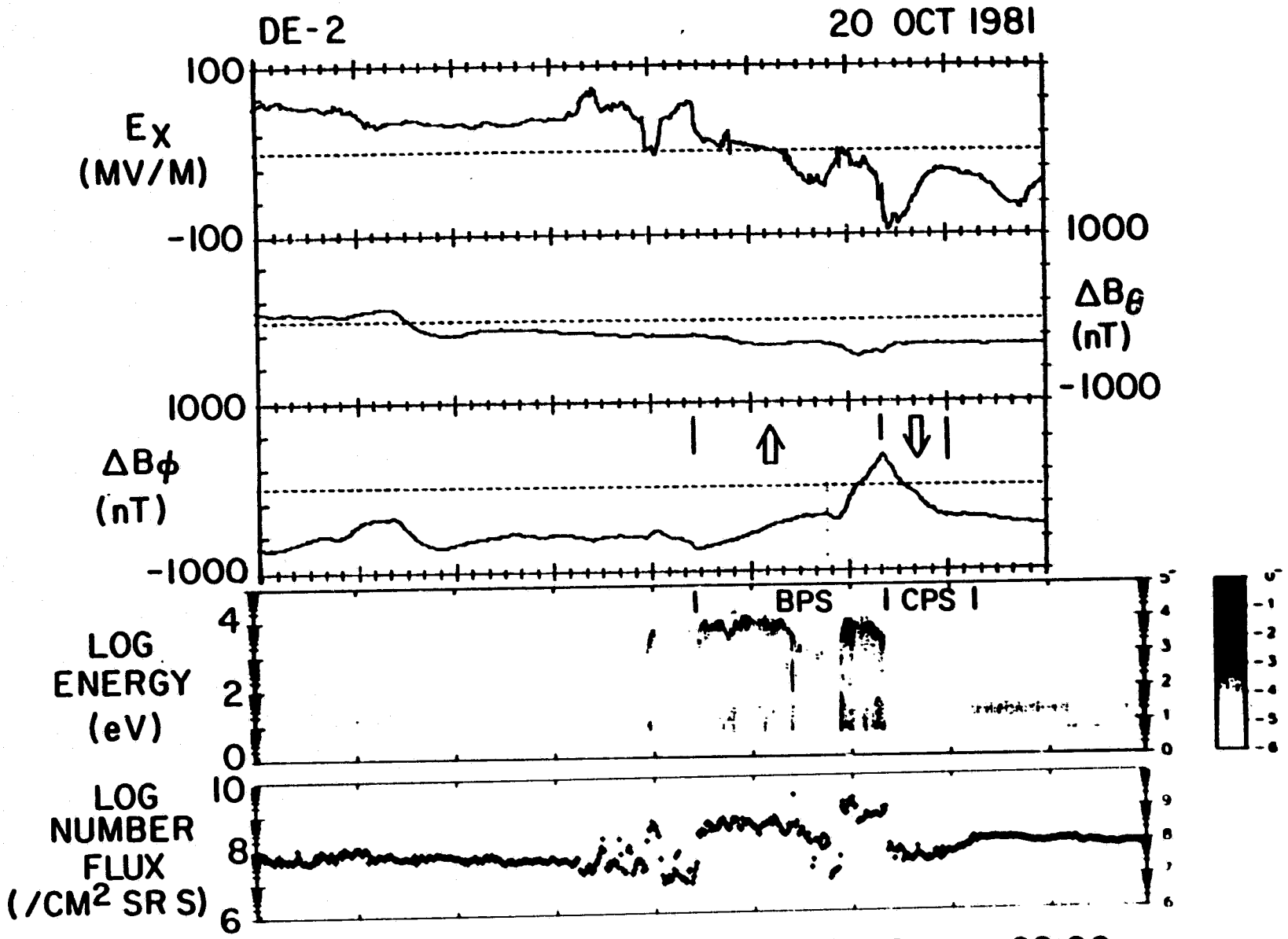


FIGURE 2

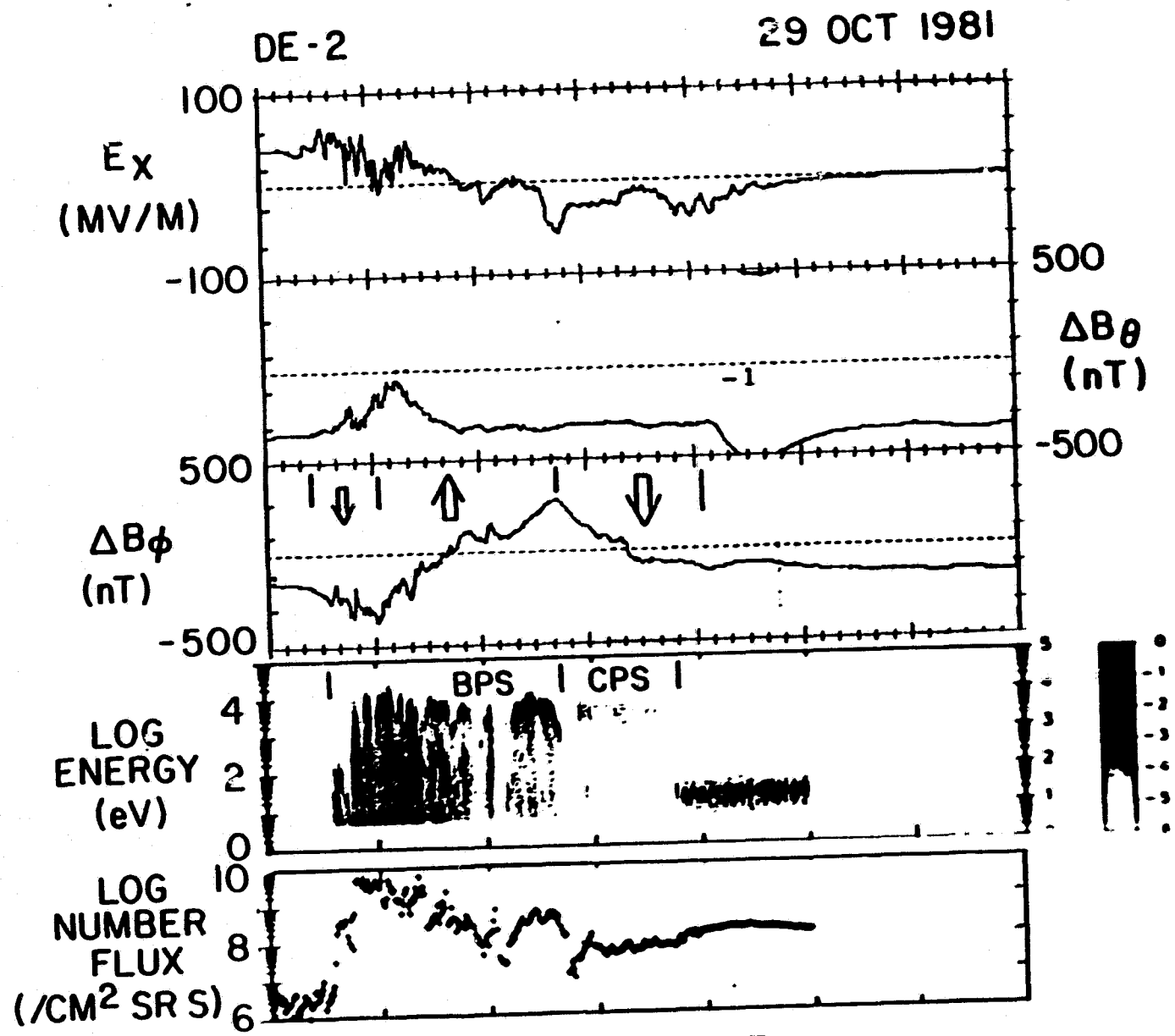


FIGURE 3

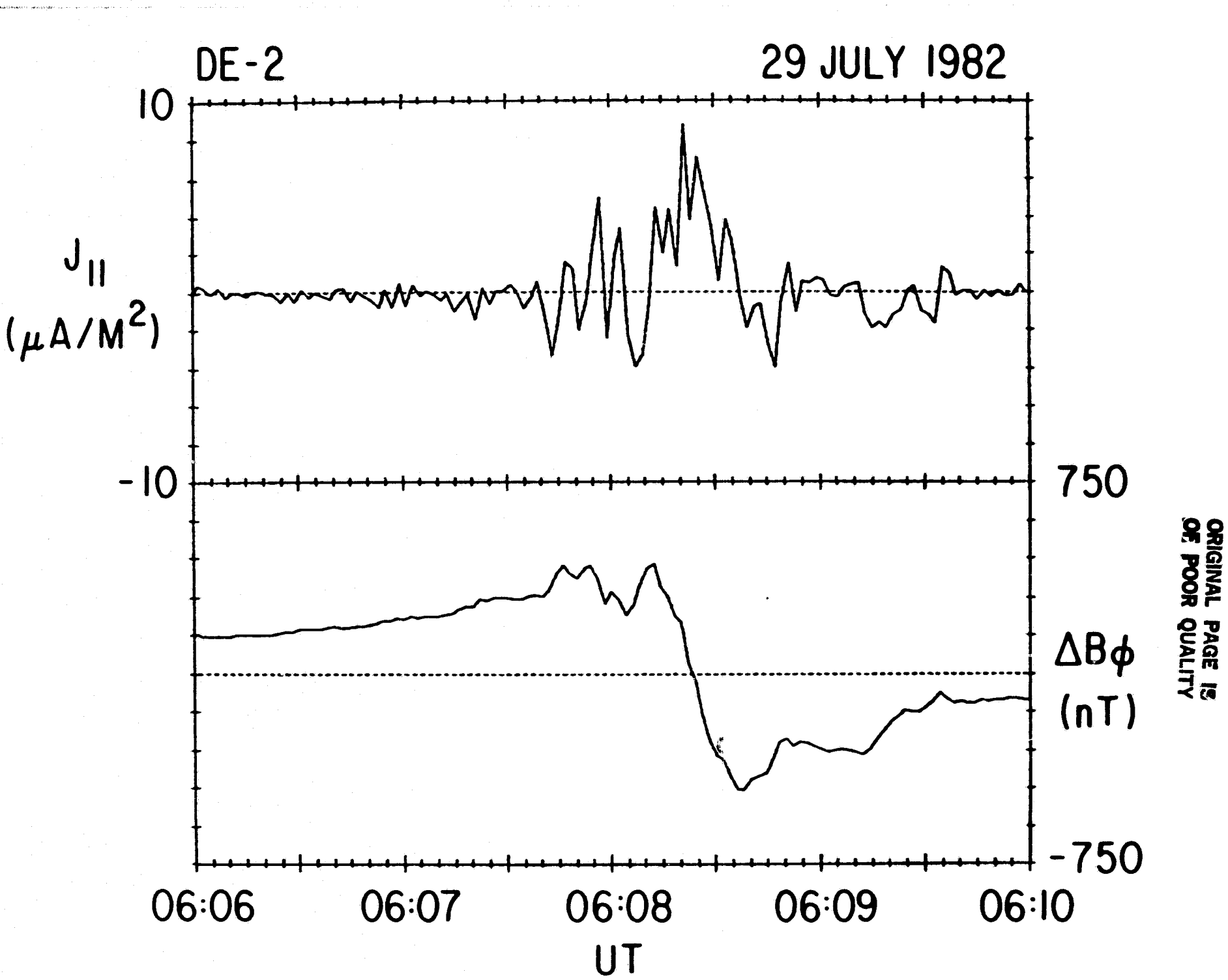




FIGURE 4

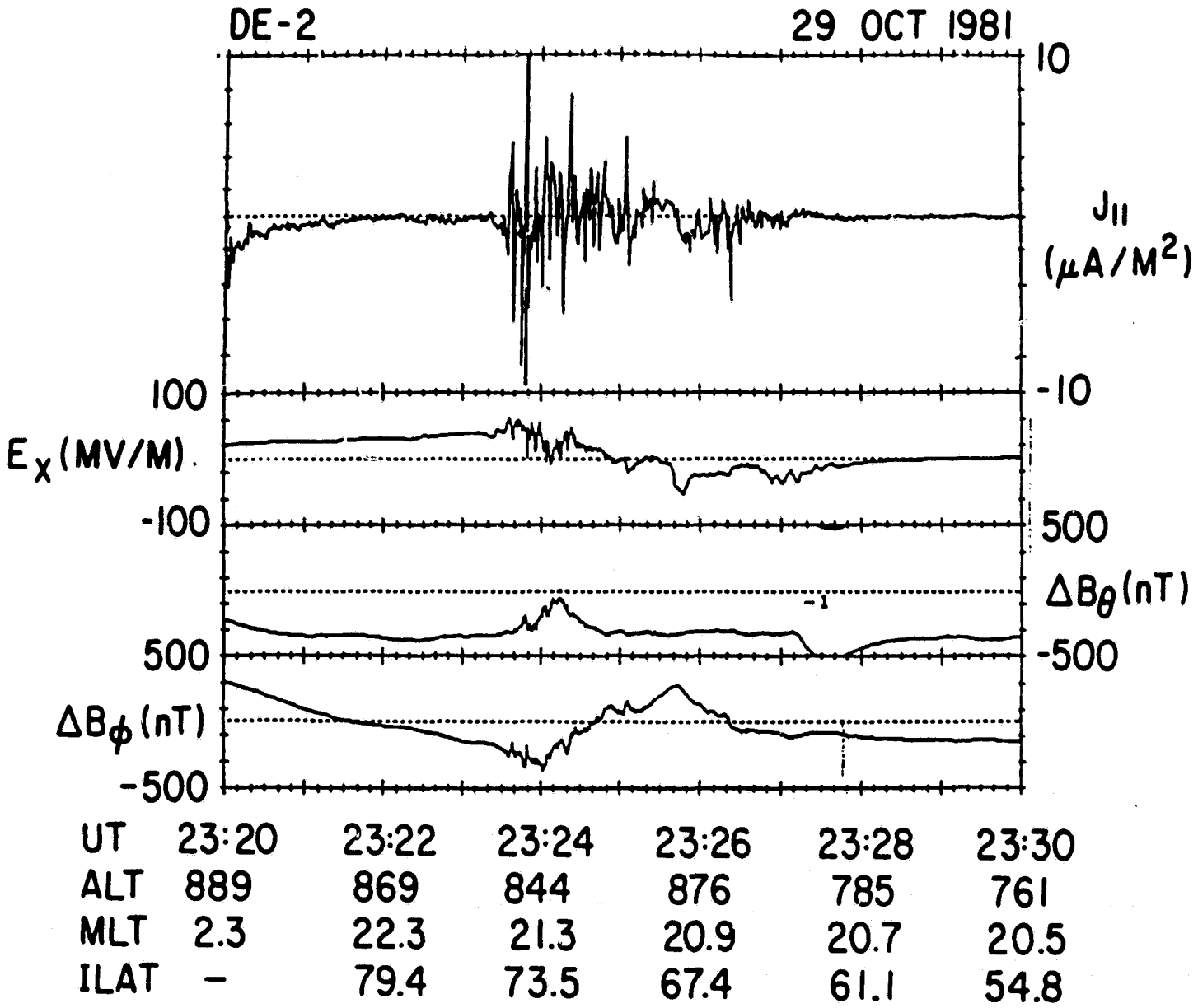


FIGURE 5

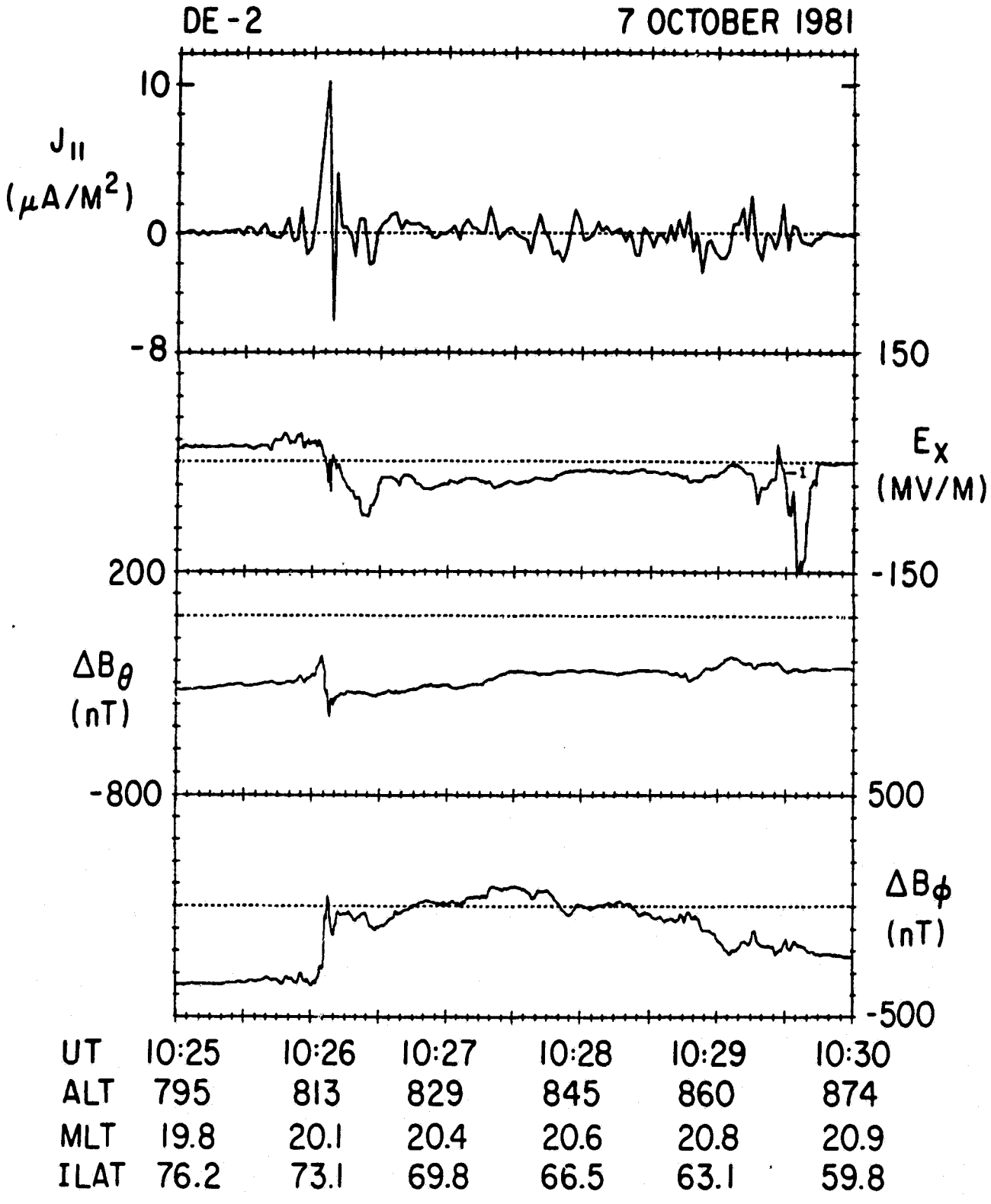


FIGURE 6

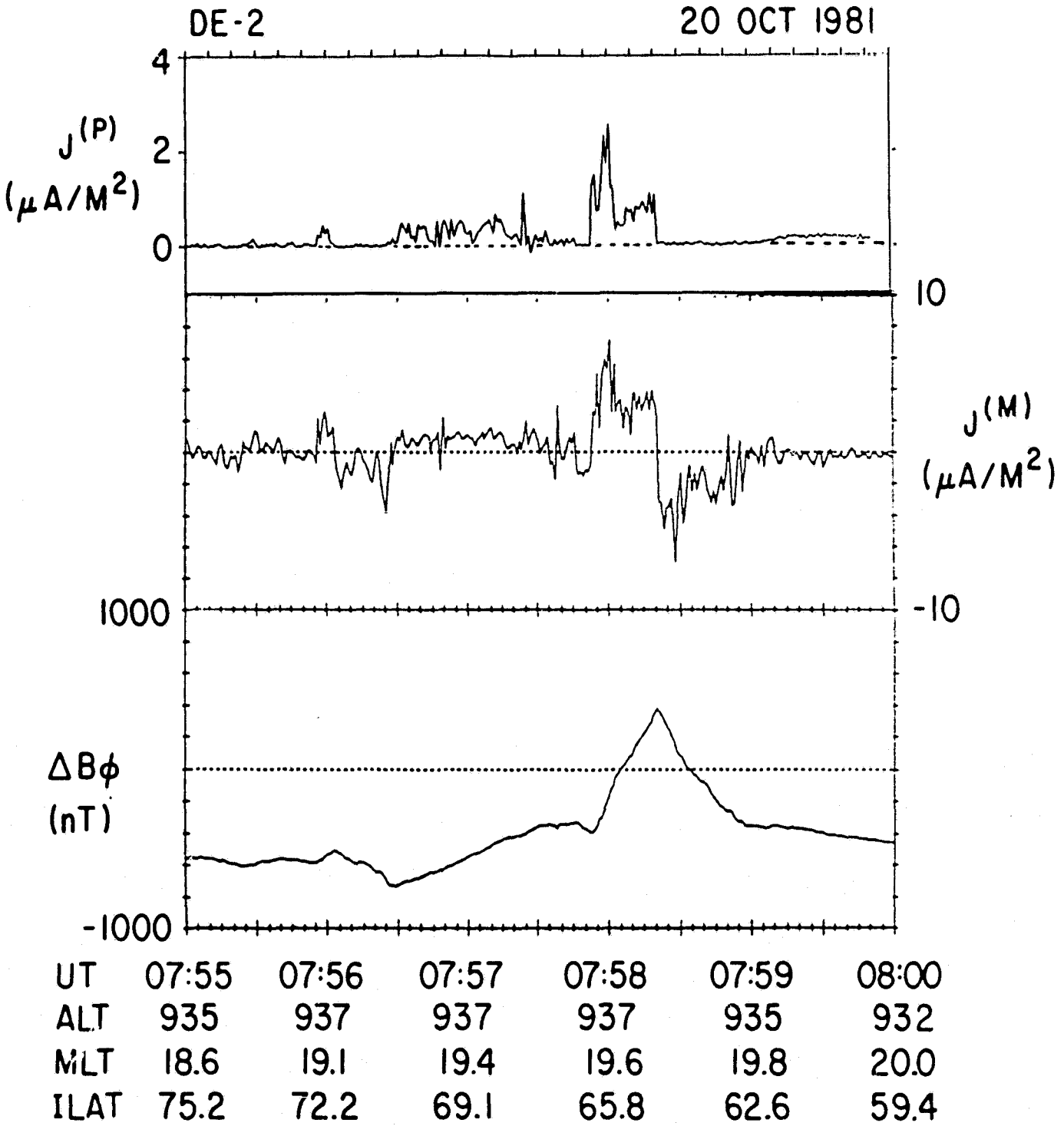


FIGURE 7